Comparative Study of CFSI, Trans-CFSI and SL-QSBI

Muhammad Awais SHARIF, Muhammad SIDDIQUE, Muhammad MUBASHER, Danish IQBAL, Gayyur HUSSAIN, Ali IMRAN

Department of Electrical Engineering, Institute of Engineering & Technology, National Fertilizer Corporation of Pakistan, PO Opposite Pak Arab Fertilizers, Khanewal Road, 60000 Multan, Pakistan

cawais300@gmail.com, msiddique@nfciet.edu.pk, mubasher4978@gmail.com, danishiqbal6050@gmail.com, ghayyur788@gmail.com, kingaliimran@gmail.com

DOI: 10.15598/aeee.v18i3.3556

Abstract. *This paper presents the comparative analysis of the three types of inverters which are Current-Fed Switched Inverter (CFSI), Trans-Current-Fed Switched Inverter (Trans-CFSI), and improved Switched Inductor-Quasi Switched Boosted Inverter (SL-QSBI). Also, a simple boost Pulse-Width-Modulation (PWM) Scheme is applied to CFSI, Trans-CFSI, and improved SL-QSBI. Each inverter category is analyzed separately for evaluating the effect of variation in duty ratio on the modulation index and boost factor. The comparisons of these inverters are rendered to quantify the voltage boost ability, voltage stress on the switching device and the voltage gain ability. Moreover, a simple boost control scheme is also modified to attain high modulation index. The efficacy of the proposed results is verified using the Saber software simulations.*

Keywords

CFSI, Pulse-Width-Modulation, SL-QSBI, Trans-CFSI.

1. Introduction

Typically, Voltage and Current Source Inverters (VSIs and CSIs individually) [1] and [2] are broadly used in electrical systems, such as solar Photovoltaic (PV) and fuel-cell applications, Un-interruptible Power Supplies (UPS) [3], wind generation systems, hybrid-electric vehicles [4] and industrial motor-drives [5], due to its high demand. Conventional VSIs are related to different major issues. They give only the voltage-buck activity of dc to ac power transformation, but the output of ac voltage can not be higher than the input of the ac source. In VSIs, shoot-through has been restricted due to Electromagnetic Interference (EMI) in power switches legs by its misgating, which affects inverter's reliability. Similarly, the current source inverter has an output of ac voltages not lower than the input of source voltage [6]. Consequently, it just gives voltage-boost activity dc to ac power transformation. Hence, an extra dc-dc converter has been added to buck-boost activities of all electrical applications, which causes a multi-stage power transformation with a higher framework volume, higher cost and complex control with lesser efficiency. By solving the issues of VSIs, the impedance-source inverters like Z-Source Inverter (ZSI) [7] and Quasi-Z-Source Inverter (QZSI) [8] were developed.

The Z-source inverter circuit is constituted by two capacitors and two inductors. Also, the advancement in the field of Z-source inverters has been rendered by different modification in Pulse-Width-Modulation (PWM) strategies [9], modeling in design according to its small ac signal analysis [10], modified structure with specified operating conditions [11] and [12]. Furthermore, in their applications, the modification in UPS output voltages [3] improves the characteristics of converter for electrical systems [13] and [14] and control methodologies, such as modified space-vector PWM [15], different control scheme [16] and [17] have been presented. Many researchers have rendered the solution of the impedance network topologies in the point of boost factor, such as enhanced boost Z-source inverter [18], Switched Inductor Z-Source Inverter (SL-ZSI) [19]. Moreover, the advancement of impedance network topologies for the achieving the lower voltage stress and lower number of passive components have been demonstrated in T-source inverter [20], Trans-Z-source inverter [21], and LCCT-Z-source inverter [22]. However, a large number of passive components are used in enhanced impedance network topologies which increase the cost, size, weight and power loss. The Switched Boost Inverters (SBIs) have been presented to minimize the cost, size, weight and power loss of the impedance source inverter topologies performed by the Z-Source Inverter (ZSI) networks.

The Watkins-Johnson topology [23] and [24] has been presented for low power applications. The characteristics of SBIs are similar to ZSIs, where the voltage is boosted by shoot-through mode. However, The SBIs have passive components lower than ZSIs and one active switch. The SBIs have two significant flaws:

- the SBIs boost factor is lesser than ZSIs,
- the current pass from the source is discontinuous because it is directly attached with a diode.

By dealing with the limitations of SBIs, the Current-Fed Switched Inverter (CFSI) has been rendered in [25]. The Current-Fed Switched Inverter (CFSI) has characteristics to enhance the boost factor and input current scenarios. The high gain CFSI operates in buck as well as boost operations. Also, the SBI has been justified in dc nanogrid applications [26] which provides a single dc input voltage that can supply ac as well as dc load simultaneously. In addition, the analysis and PWM control strategy of the SBI have been demonstrated in [27]. In [28], class of quasi-Switched Boost Inverters (qSBIs) has also been elaborated to solve the drawbacks of SBIs. It offers several advantages over SBI, including increasing the boost voltage factor, reducing capacitor voltage stress and improving input current scenario.

The coupled inductors based high boost inverter has been proposed [29], named as improved Trans-CFSI which provides higher gain characteristics. To enhance dc voltage gain as well as low input current ripple, the Switched-Inductor Quasi-Switched Boost Inverter (SL-QSBI) has been rendered in [30]. Additionally, an Actively Switched Capacitor/Switched Inductor Z-Source Inverter (ASC/SL-ZSI) has also been demonstrated in [31]. This paper presents a modified simple boost control strategy that applied to CFSI, Improved SL-QSBI and Trans-CFSI. The CFSI, trans-CFSI and Improved SL-QSBI are describing some similarities according to its schematic diagrams, operation modes and their results.

2. Review on Switched Boost Inverter [23] and [24]

The Switched Boost Inverter (SBI) has the single-stage power conversion over ZSIs, including the lesser passive components count and also has the additional ability of active components. The circuit included one inductor (L_a), one capacitor (C), two diodes (D_a, D_b) and one active switch (S). The output of SBIs is made smooth by the low pass (L_c) filter. Figure 1(a) shows the circuit schematic of SBIs. The circuit operates in shoot-through and non-shoot-through states.

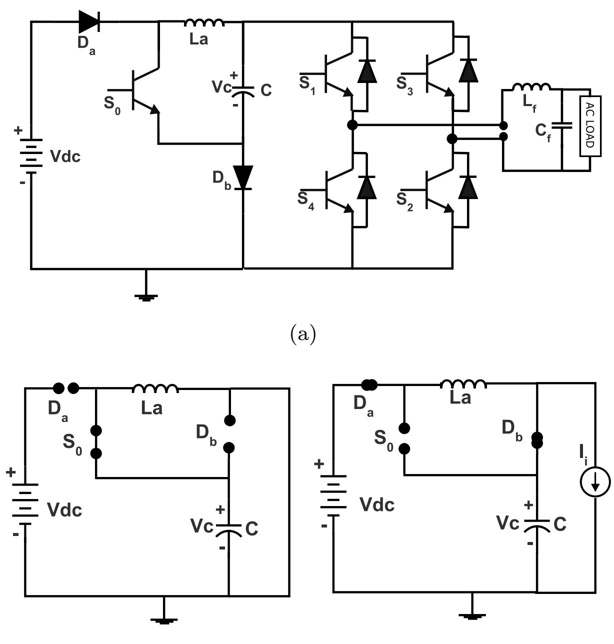

Fig. 1: (a) Switched Boost Inverter, (b) Shoot-Through State Of Switched Boost Inverter and (c) Non-Shoot-Through State Of Switched Boost Inverter.

In shoot-through state, an active switch (S) is open, the diodes (D_a, D_b) blocks the current which are in reverse-biased state and the inductor is getting charged through the voltages of capacitor as shown in Fig. 1(b).

$$V_L = V_C, \tag{1}$$

$$I_C = -I_L. \tag{2}$$

In non-shoot-through state, the diodes (D_a, D_b) become forward biased and supply power to the inverter, as shown in Fig. 1(c).

$$V_L = V_{DC} - V_C, \tag{3}$$

$$I_C = I_L - I_i. \tag{4}$$

By applying volt–second balance, we get:

$$(V_C)(D) = (V_{DC} - V_C)(1 - D). \tag{5}$$

By solving Eq. (5), we get:

$$\frac{V_C}{V_{DC}} = \frac{(1 - D)}{(1 - 2D)}, \tag{6}$$

$$B_{SBIs} = \frac{(1-D)}{(1-2D)}. \quad (7)$$

From Eq. (7), it can be observed that the boost factor characteristics of SBI become unity in $D = 0$ condition, and turn higher when $D = 0.5$. Moreover, the voltage gain of SBIs is $1 - D$ time over ZSIs.

3. Current-Fed Switched Inverter

The Current-Fed Switched Inverter (CFSI) topology [25] has been derived with the combination of ZSIs and SBIs. The CFSI circuit schematic shown in Fig. 2(a), which is the single-phase SBI topology. The CFSI included one inductor (L_a), capacitor (C), two diodes (D_a, D_b), a controlled switch (S) and inverter bridge. In the CFSI, the input dc source is coupled with the inductor which draws the continuous current.

In CFSI, the shoot-through operation is also involved, like in SBIs and ZSIs, but it improves EMI noise immunity. It can work in both boost and buck mode which is reliable for renewable applications.

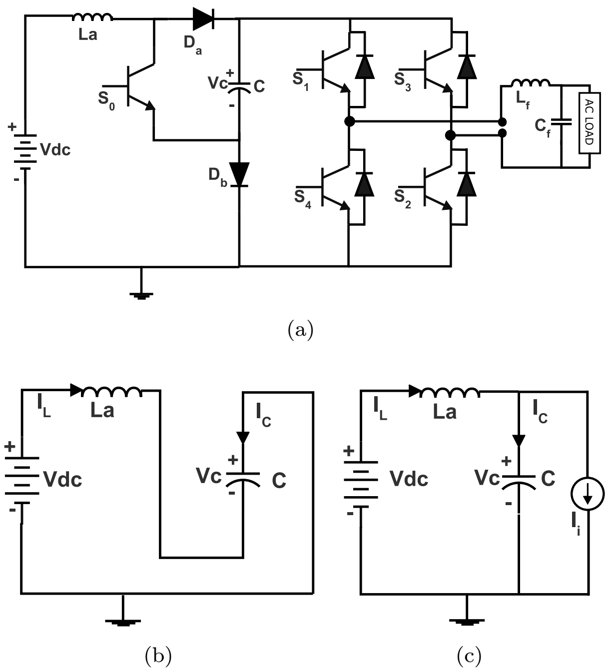

Fig. 2: (a) CFSI, (b) Shoot-Through State Of CFSI and (c) Non-Shoot-Through State Of CFSI.

3.1. Steady-State Operation of CFSI

The schematic of CFSI is shown in Fig. 2(a). Similarly, the circuit operates in shoot-through and non-shoot-through states as SBIs. In case of shoot-through state, an active switch (S) is open with inverter legs, and the diodes (D_a, D_b) become reverse biased. The DC input voltage with capacitor voltage charges the inductor which is displayed in Fig. 2(b).

By applying KVL:

$$-V_{DC} + V_L - V_C = 0, \quad (8)$$

$$V_L = V_{DC} + V_C, \quad (9)$$

$$I_C = -I_L. \quad (10)$$

In case of non-shoot-through interval, an active switch (S) and inverter legs are off, and the diodes (D_a, D_b) become forward biased. The inductor charges and transfers power to the ac load through the inverter bridge.

By applying KVL:

$$V_L - V_{DC} + V_C = 0, \quad (11)$$

$$V_L = V_{DC} - V_C, \quad (12)$$

$$I_C = I_L - I_i. \quad (13)$$

In case of non-shoot-through state, the inverter operates in power interval as well as zero intervals, as displayed in Fig. 2(b).

By applying volt–second balance, we get:

$$(V_{DC} + V_C)(D) + (V_{DC} - V_C)(1-D) = 0, \quad (14)$$

$$(V_{DC} + V_C)(D) = -(V_{DC} - V_C)(1-D). \quad (15)$$

By solving the Eq. (15), we get:

$$V_{DC} = V_C(1-2D), \quad (16)$$

$$\frac{V_C}{V_{DC}} = \frac{1}{(1-2D)}, \quad (17)$$

$$B_{CFSI} = \frac{1}{(1-2D)}. \quad (18)$$

Therefore, Eq. (18) represents the boost factor of CFSI.

4. Trans-CFSI

The Trans-CFSI topology [29] is obtained from current-fed switched inverter topology. The Trans-CFSI circuit schematic is shown in Fig. 3(a) which is the single-phase SBI topology. The Trans- CFSI includes the two coupled inductor (L_a, L_b), capacitor (C), two diodes (D_a, D_b), a controlled switch (S) and inverter bridge. The inductor is attached with input dc source which draws the continuous current. In Trans-CFSI, the coupled inductors used to attain high gain and boost characteristics.

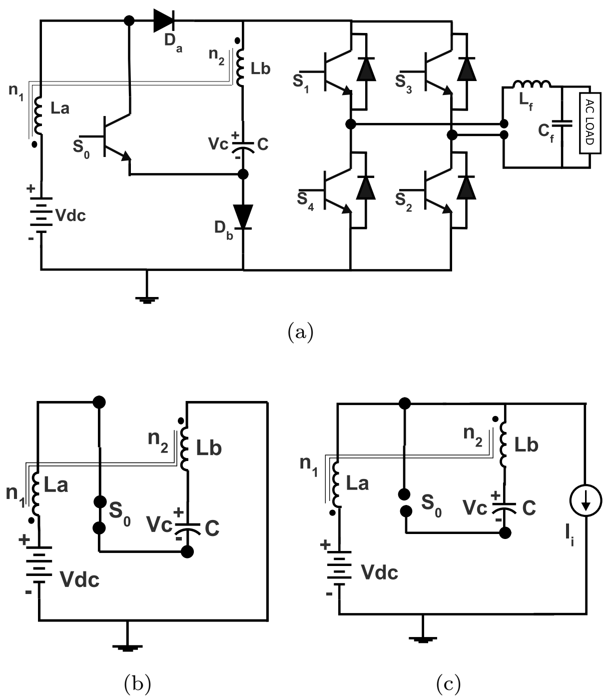

Fig. 3: (a) Trans-CFSI, (b) Shoot-Through State Of Trans-CFSI and (c) Non-Shoot-Through State Of Trans-CFSI.

4.1. Steady-State Operation of Trans-CFSI

The schematic of Trans-CFSI is shown in Fig. 3(a). The coupled inductors work as a transformer by adjusting its turn ratio (N_p and N_s). The primary number of turns (N_p) is higher than the secondary number of turns (N_s) for better operation of the inverter. Similarly, the circuit also operates in shoot-through and non-shoot-through states as CFSI.

In case of shoot-through interval, an active switch (S) is on with inverter switch pair, and the diodes (D_a, D_b) become reverse biased due to reverse voltage, as shown in Fig. 3(b).

By applying KVL,we get:

$$V_{La} = V_{DC} + V_C + V_{Lb}, \tag{19}$$

$$V_{Lb} = \frac{n_2}{n_1} V_{La} = nV_{La} = \frac{n(V_{DC} + V_C)}{(1-n)}, \tag{20}$$

$$I_C = -I_{La}. \tag{21}$$

In case of non-shoot-through interval, an active switch (S) and inverter legs are off, the diodes (D_a, D_b) become forward biased. In addition, the inverter operates in power interval as well as zero intervals. In power state, the inverter supplies power to ac load; and in zero interval, the inverter becomes free or open circuit, as shown in Fig. 3(c).

$$V_{La} + V_{Lb} = V_{DC} - V_C, \tag{22}$$

$$V_{Lb} = \frac{n_2}{n_1} V_{La} = nV_{La} = \frac{(n(V_{DC} - V_C))}{(1+n)}. \tag{23}$$

By applying volt–second balance, we get:

$$\frac{n(V_{DC} + V_C)}{(1-n)}(D) + \frac{(n(V_{DC} - V_C))}{(1+n)}(1-D) = 0, \tag{24}$$

$$\frac{n(V_{DC} + V_C)}{(1-n)}(D) = -\frac{(n(V_{DC} - V_C))}{(1+n)}(1-D), \tag{25}$$

$$\frac{V_C}{V_{DC}} = \frac{1}{1 - \dfrac{2D}{(1-n)}}, \tag{26}$$

$$B_{Trans-CFSI} = \frac{1}{1 - \dfrac{2D}{(1-n)}}. \tag{27}$$

5. Improved SL-QSBI

The improved SL-QSBI inverter topology is represented in Fig. 4(a). The improved SL-QSBI topology is the advancement in current-fed switched inverter topology. The circuit included SL cell in the CFSI topology which improves the dc voltage gain. It consists of two inductors (L_a, L_b), capacitor (C), five diodes $(D_1, D_2, D_3, D_a, D_b)$, a controlled switch (S) and inverter bridge. Due to SL cell, the input current profile is continuous.

5.1. Steady-state Operation of Improved SL-QSBI

The schematic of improved SL-QSBI is shown in Fig. 4(a). Similarly, as the CFSI and Trans-CFSI, the circuit operates in shoot-through and non-shoot-through states. In case of shoot-through interval, an active switch (S) is on with inverter switch pair, and the diodes (D_1, D_2) are on where $(D_a, D_b$ and $D_3)$ are not in conduction. The inductors are getting charged through input dc and capacitor voltages. The inductor voltages will be parallel, as shown in Fig. 4(b).

So,

$$V_L = V_{La} + V_{Lb}. \tag{28}$$

By applying KVL:

$$V_L - V_{DC} - V_C = 0, \tag{29}$$

$$V_L = V_{DC} + V_C, \tag{30}$$

$$i_C = -(i_{La} + i_{Lb}), \tag{31}$$

$$V_{IN} = 0. \tag{32}$$

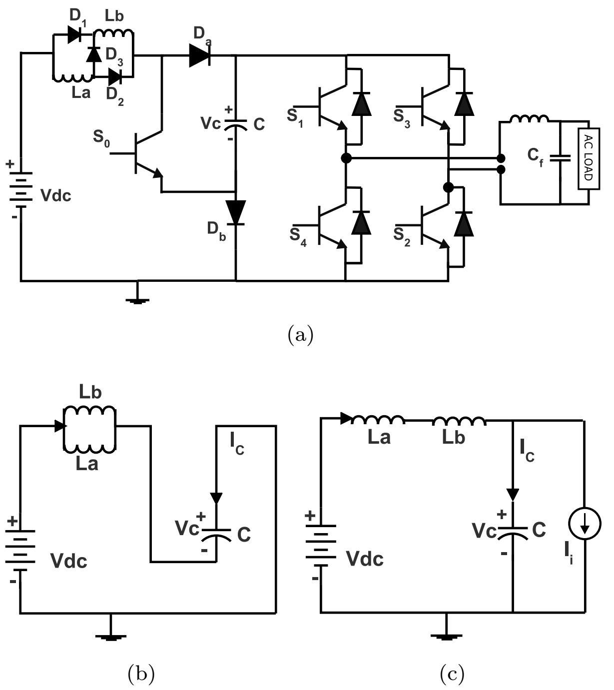

Fig. 4: (a) Improved SL-QSBI, (b) Shoot-Through State Of Improved SL-QSBI and (c) Non-Shoot-Through state of Improved SL-QSBI.

In case of non-shoot-through interval, an active switch (S) is off with inverter switch pair, and the diodes (D_1, D_2) are off while the diodes $(D_a, D_b$ and $D_3)$ are in conduction. The inverter operates in power state, which means inverter supplies power to the load. During this state, the inductors $(L_a$ and $L_b)$ are in series and capacitor is charged, as shown in Fig. 4(c).

$$+2V_{La} - V_{DC} + V_C = 0, \tag{33}$$

$$V_{La} = \frac{(V_{DC} - V_C)}{2}. \tag{34}$$

By applying volt–second balance, we get:

$$(V_{DC} + V_C)(D) = \frac{(V_{DC} - V_C)}{2}(1 - D). \tag{35}$$

By solving Eq. (35), we get:

$$\frac{V_C}{V_{DC}} = \frac{(1 + D)}{(1 - 3D)}, \tag{36}$$

$$B_{SL-QSBI} = \frac{(1 + D)}{(1 - 3D)}. \tag{37}$$

6. PWM Control Scheme

Simple Boost Control (SBC) scheme is the basic method of inverter's control schemes, which is simple and easy to be implemented. SBC is explored and utilized by many researchers e.g., in CFSI [25] and Trans-CFSI [29], the traditional sine-triangular Pulse-Width-Modulation (PWM) with unipolar voltage switching was used. Moreover, SL-SBI [31] describes the three-phase simple boost Pulse-Width-Modulation (PWM) control scheme. Likewise the CFSI [25], the simple boost control method is illustrated in Fig. 5.

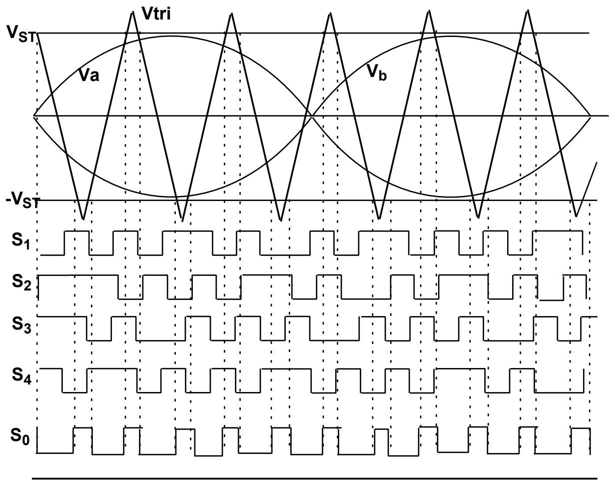

Fig. 5: Simple Boost PWM Scheme.

The simple boost method is used to control the time of the shoot-through state. The PWM scheme represents the signals (S_1, S_2, S_3, S_4) which is generated by comparing triangular waves with two sinusoidal waveforms. The (S_0) signals are generated by comparing the two constant voltages and triangular waveforms. The main work of the (S_0) signal is to generate the shoot-through in the inverter bridge. The switching frequency of this PWM control scheme has also been modified according to its power loss, EMI noise and efficiency. In this paper, a simple boost Pulse-Width-Modulation (PWM) scheme is applied to CFSI, Trans-CFSI and improved SL-QSBI.

7. Comparison of CFSI, Trans-CFSI and Improved SL-QSBI

The CFSI, Trans-CFSI and improved SL-QSBI are related to each other by its working module and operating modes. All have included the shoot-through state in their boosting control method. By applying the modified simple boost control scheme, the comparison is related to their boost factor, modulation index, their input current profiles and their voltage gain.

7.1. Boost Factor

The boost factors of the CFSI, Trans-CFSI and improved SL-QSBI inverters are shown in Eq. (38), Eq. (39) and Eq. (40).

$$B_{CFSI} = \frac{1}{(1-2D)}, \tag{38}$$

$$B_{Trans-CFSI} = \frac{1}{1-\dfrac{2D}{(1-n)}}, \tag{39}$$

$$B_{SL-QSBI} = \frac{(1+D)}{(1-3D)}. \tag{40}$$

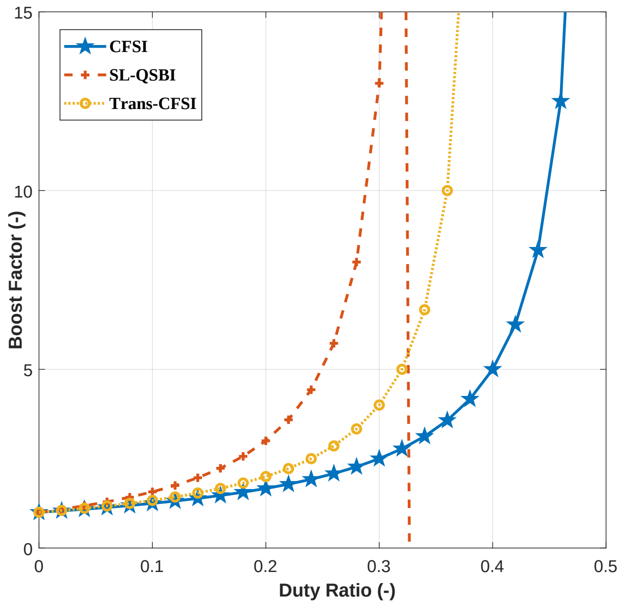

Fig. 6: Boost Factor Versus Duty Ratio.

The boost factor comparison is represented in Fig. 6 with respect to their duty ratio. From the equations, it is clear that if the duty ratio is low, the boost factor is high. And if the duty ratio is high, the boost factor is low. Moreover, it affects the voltage gain and performance parameter. The duty ratio of CFSI, Trans-CFSI and improved SL-QSBI inverters has been decreased and it increases their boost factor through simple boost Pulse-Width-Modulation (PWM) scheme, as shown in Fig. 6.

The graph shows that improved SL-QSBI has a high boost factor and the smallest duty ratio. Therefore, the improved SL-QSBI has higher gain than CFSI and Trans-CFSI.

7.2. Voltage Gain

The Equation (43), Eq. (44) and Eq. (45) represent the modulation indexes which are derived for the CFSI, Trans-CFSI and improved SL-QSBI. The modulation index comparison is represented in Fig. 7 with respect to their voltage gain. The equations represent that if the modulation index is low, the voltage gain is low. And if the modulation index is high, the voltage gain is high. The lowest modulation index affects the power characteristics of inverters. In Fig. 7, the simple boost Pulse-Width-Modulation (PWM) scheme increases modulation index and voltage gain ability of CFSI, Trans-CFSI and improved SL-QSBI. The significant characteristics help to make the system reliable and efficient.

$$G = M \cdot B, \tag{41}$$

and

$$B = 1 - M. \tag{42}$$

By following the Eq. (41) and Eq. (42), we get the gain of CFSI, Trans-CFSI and improved SL-QSBI.

$$G = \frac{M}{(2M-1)}, \tag{43}$$

$$G = \frac{M}{(n^2 - 2Mn + 2M - 1)}, \tag{44}$$

$$G = \frac{(2M - M^2)}{(3M-2)}. \tag{45}$$

The graph shows that SL-QSBI has a high voltage gain and the smallest modulation index. Therefore, the SL-QSBI has higher gain than CFSI and Trans-CFSI.

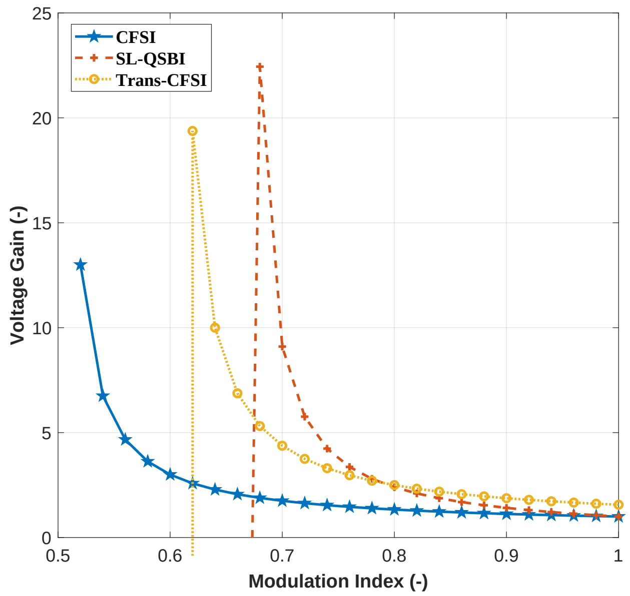

Fig. 7: Voltage Gain Versus Modulation Index.

7.3. Voltage Stress

The voltage stress comparison is represented in Fig. 8 with respect to their voltage gain. If the voltage stress is low, then the voltage gain is high. And if the voltage stress is high, then the voltage gain is low. The voltage stress of CFSI, Trans-CFSI and improved SL-QSBI has been reduced through simple boost Pulse-Width-Modulation (PWM) scheme, as shown in Fig. 8.

The graph shows that improved SL-QSBI has a high voltage gain and the smallest voltage stress. Therefore, the improved SL-QSBI has a higher gain than CFSI and Trans-CFSI.

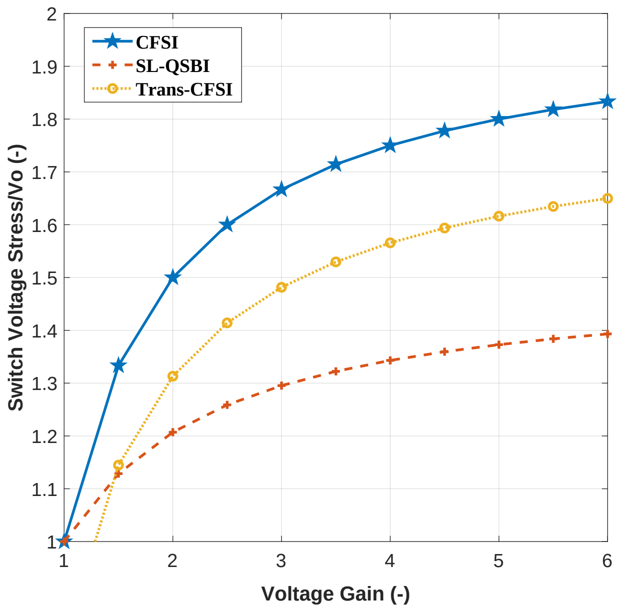

Fig. 8: Voltage Gain Versus Voltage Stress.

7.4. Input Current Profiles

In ZSI and SBI the diodes are connected in series with the input dc voltage. Therefore, it can draw the discontinuous current in the circuit which reduces the life of the inverter applications. So, the inductor is attached with input dc source which draws continuous current. The CFSI, Trans-CFSI and improved SL-QSBI work on the continuous current property which increases the life of renewable applications.

8. Simulation Results

By using the simple boost control method, the performance of all of the three inverter topologies has been simulated. Figure 5 shows the PWM scheme and the configuration of all of the three implemented inverter topologies. The circuit parameters are shown in Tab. 1.

Simulations are performed by the saber software which is quite easy to display and perform the results. The simulation results of all three circuits are shown in Fig. 9, Fig. 10 and Fig. 11, which display the simulation with respect to the dc link voltage (V_{pn}), output line-to-line voltage (V_{out}) and the inductor current ($I_{La,b}$) of all the three inverters with different operational conditions.

Tab. 1: Circuit Parameters Used For Simulation.

Attributes	CFSI	Trans-CFSI	SL-QSBI
Input Voltage	40 V	40 V	40 V
Modulation Frequency (f)	50 Hz	50 Hz	50 Hz
Switching Frequency (f_s)	9 kHz	9 kHz	9 kHz
Inductor (L_a, L_b)	4.9 mH	8.13 mH, 516 µH, $n = 0.26$ 5.13 mH, 420 µH, $n = 0.29$	4.7 mH, 495 µH
Capacitor (C)	780 µF	640 µF	980 µF
Output Filter Capacitor (C_f)	8.3 µF	8.3 µF	8.3 µF
Output Filter Inductor (L_f)	4.9 mH	4.9 mH	4.9 mH

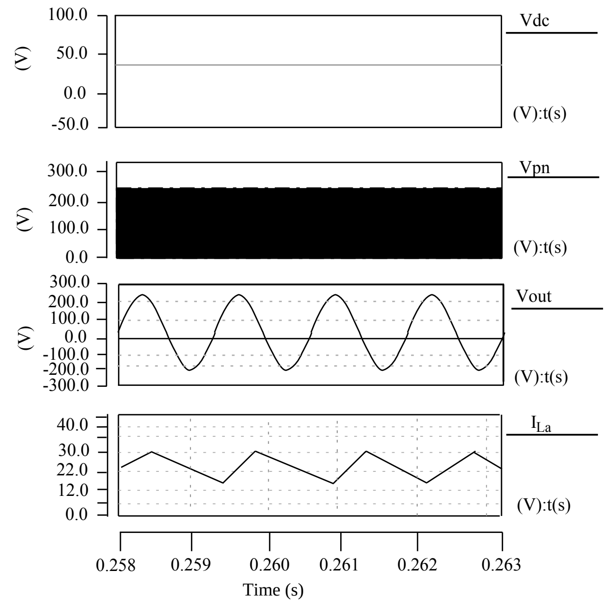

Fig. 9: Output Waveform of CFSI.

In case of CFSI, the output voltage is 220 and $V_{pn} = 232$, as shown in Fig. 9. The output voltage of Trans-CFSI is 220 and $V_{pn} = 210$ is shown in Fig. 10.

In Fig. 11, the output voltage of improved SL-QSBI is 220 with $V_{pn} = 195$. From the simulations results, it is seen that the V_{pn} of improved SL-QSBI is lower than the other two inverters.

Therefore, the improved SL-QSBI has the ability of 0.3 duty ratio, which makes the modulation index near to 0.7 and higher than the other two inverter topologies. As a result, the voltage stress on the switching devices of inverters will decrease when compared with other topologies. The improved SL-SBIs obtain better gain than the other two inverter topologies on 0.7 value of modulation index. It is important to mention that the presented inverter topologies are useful for many real-world inverter applications, such as photo-voltaic power systems, fuel cells based power systems and other renewable energy-based power systems.

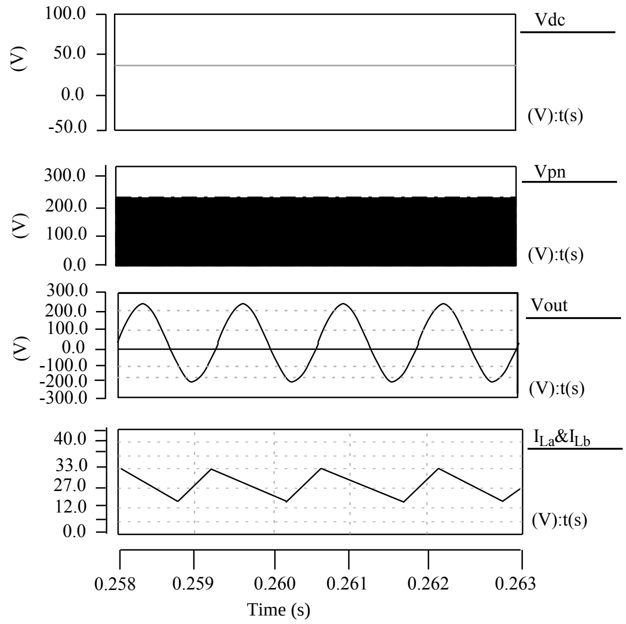

Fig. 10: Output Waveform of Trans-CFSI.

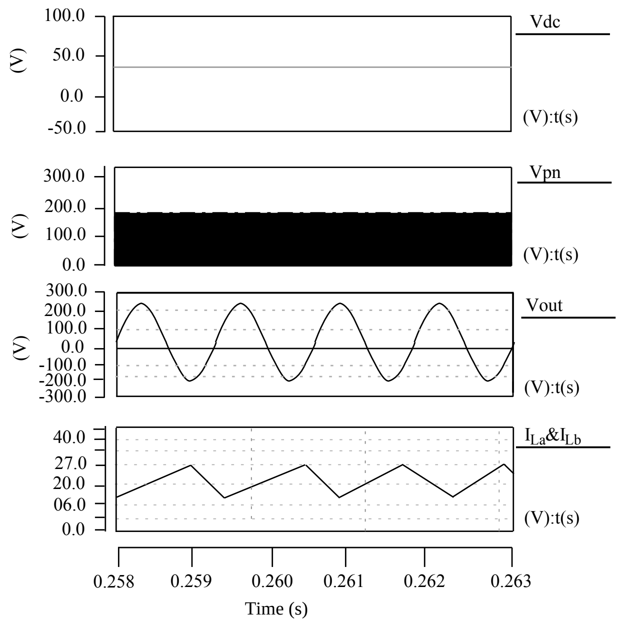

Fig. 11: Output Waveform of Improved SL-QSBI.

9. Conclusion

This paper represents the comparisons of three circuit topologies using a simple boost Pulse-Width-Modulation (PWM) scheme. The presented scheme obtains a smaller duty ratio of the improved SL-QSBI than CFSI and Trans-CFSI for the required output voltage. The improved SL-QSBI also achieves a good modulation index to attain better voltage quality. The voltage gain characteristics of the improved SL-QSBI are higher than CFSI and Trans-CFSI. The voltage stress on the switching devices of CFSI,Trans-CFSI and improved SL-QSBI has been reduced. Simulations were used for presenting the efficacy of the proposed scheme.

References

[1] HUANG, H. and P. A. MAWBY. A Lifetime Estimation Technique for Voltage Source Inverters. *IEEE Transactions on Power Electronics*. 2013, vol. 28, iss. 8, pp. 4113–4119. ISSN 1941-0107. DOI: 10.1109/TPEL.2012.2229472.

[2] KAVIMANDAN, A. and S. P. DAS. Control and protection strategy for a three-phase single-stage boost type grid-connected current source inverter for PV applications. In: *IEEE International Conference on Industrial Technology (ICIT)*. Cape Town: IEEE, 2013, pp. 1722–1727. ISBN 978-1-4673-4569-9. DOI: 10.1109/ICIT.2013.6505935.

[3] UTHIRASAMY, R., U. S. RAGUPATHY and V. K. CHINNAIYAN. Structure of boost DC-link cascaded multilevel inverter for uninterrupted power supply applications. *IET Power Electronics*. 2015, vol. 8, iss. 11, pp. 2085–2096. ISSN 1755-4535. DOI: 10.1049/iet-pel.2014.0746.

[4] HONG, J., H. LEE and K. NAM. Charging method for the second battery in dual inverter drive systems for electric vehicles. In: *IEEE Applied Power Electronics Conference and Exposition - APEC 2014*. Fort Worth: IEEE, 2014, pp. 2407–2414. ISBN 978-1-4799-2325-0. DOI: 10.1109/APEC.2014.6803640.

[5] TRABELSI, M., M. BOUSSAK and A. CHAARI. High performance single and multiple faults diagnosis in voltage source inverter fed induction motor drives. In: *XXth International Conference on Electrical Machines*. Marseille: IEEE, 2012, pp. 1717–1723. ISBN 978-1-4673-0142-8. DOI: 10.1109/ICElMach.2012.6350112.

[6] RASHID, M. H. Power Electronics: Circuits, Devices, and Applications. 2nd ed. Englewood Cliffs: Prentice-Hall, 1993. ISBN 978-0-1367-8996-3.

[7] PENG, F. Z. Z-source inverter. *IEEE Transactions on Industry Applications*. 2003, vol. 39, iss. 2, pp. 504–510. ISSN 1939-9367. DOI: 10.1109/TIA.2003.808920.

[8] ANDERSON, J. and F. Z. PENG. Four quasi-Z-Source inverters. In: *IEEE Power Electronics Specialists Conference*. Rhodes: IEEE, 2008, pp. 2743–2749. ISBN 978-1-4244-1667-7. DOI: 10.1109/PESC.2008.4592360.

[9] TANG, Y., S. XIE and J. DING. Pulsewidth Modulation of Z-Source Inverters With Minimum Inductor Current Ripple. *IEEE Transactions on Industrial Electronics*. 2014, vol. 61, iss. 1, pp. 98–106. ISSN 1557-9948. DOI: 10.1109/TIE.2013.2240632.

[10] LIU, J., J. HU and L. XU. Dynamic Modeling and Analysis of Z Source Converter—Derivation of AC Small Signal Model and Design-Oriented Analysis. *IEEE Transactions on Power Electronics*. 2007, vol. 22, iss. 5, pp. 1786–1796. ISSN 1941-0107. DOI: 10.1109/TPEL.2007.904219.

[11] RAJAKARUNA, S. and L. JAYAWICKRAMA. Steady-State Analysis and Designing Impedance Network of Z-Source Inverters. *IEEE Transactions on Industrial Electronics*. 2010, vol. 57, iss. 7, pp. 2483–2491. ISSN 1557-9948. DOI: 10.1109/TIE.2010.2047990.

[12] SHEN, M. and F. Z. PENG. Operation Modes and Characteristics of the Z-Source Inverter With Small Inductance or Low Power Factor. *IEEE Transactions on Industrial Electronics*. 2008, vol. 55, iss. 1, pp. 89–96. ISSN 1557-9948. DOI: 10.1109/TIE.2007.909063.

[13] ROSAS, C. J. C., F. Z. PENG, H. CHA and C. ROGERS. Z-Source-Converter-Based Energy-Recycling Zero-Voltage Electronic Loads. *IEEE Transactions on Industrial Electronics*. 2009, vol. 56, iss. 12, pp. 4894–4902. ISSN 1557-9948. DOI: 10.1109/TIE.2009.2026374.

[14] VINNIKOV, D. and I. ROASTO. Quasi-Z-Source-Based Isolated DC/DC Converters for Distributed Power Generation. *IEEE Transactions on Industrial Electronics*. 2011, vol. 58, iss. 1, pp. 192–201. ISSN 1557-9948. DOI: 10.1109/TIE.2009.2039460.

[15] TRAN, Q.-V., T.-W. CHUN, J.-R. AHN and H.-H. LEE. Algorithms for Controlling Both the DC Boost and AC Output Voltage of Z-Source Inverter. *IEEE Transactions on Industrial Electronics*. 2007, vol. 54, iss. 5, pp. 2745–2750. ISSN 1557-9948. DOI: 10.1109/TIE.2007.895146.

[16] GAJANAYAKE, C. J., D. M. VILATHGAMUWA and P. C. LOH. Development of a Comprehensive Model and a Multiloop Controller for Z-Source Inverter DG Systems. *IEEE Transactions on Industrial Electronics*. 2007, vol. 54, iss. 4, pp. 2352–2359. ISSN 1557-9948. DOI: 10.1109/TIE.2007.894772.

[17] SHEN, M., J. WANG, A. JOSEPH, F. Z. PENG, L. M. TOLBERT and D. J. ADAMS. Constant boost control of the Z-source inverter to minimize current ripple and voltage stress. *IEEE Transactions on Industry Applications*. 2006, vol. 42, iss. 3, pp. 770–778. ISSN 1939-9367. DOI: 10.1109/TIA.2006.872927.

[18] LI, D., P. C. LOH, M. ZHU, F. GAO and F. BLAABJERG. Enhanced-Boost Z-Source Inverters With Alternate-Cascaded Switched and Tapped-Inductor Cells. *IEEE Transactions on Industrial Electronics*. 2013, vol. 60, iss. 9, pp. 3567–3578. ISSN 1557-9948. DOI: 10.1109/TIE.2012.2205352.

[19] ZHU, M., K. YU and F. L. LUO. Switched Inductor Z-Source Inverter. *IEEE Transactions on Power Electronics*. 2010, vol. 25, iss. 8, pp. 2150–2158. ISSN 1941-0107. DOI: 10.1109/TPEL.2010.2046676.

[20] STRZELECKI, R., M. ADAMOWICZ, N. STRZELECKA and W. BURY. New type T-Source inverter. In: *Compatability and Power Electronics*. Badajoz: IEEE, 2009, pp. 191–195. ISBN 978-1-4244-2855-7. DOI: 10.1109/CPE.2009.5156034.

[21] QIAN, W., F. Z. PENG and H. CHA. Trans-Z-source inverters. In: *The 2010 International Power Electronics Conference - ECCE ASIA*. Sapporo: IEEE, 2010, pp. 1874–1881. ISBN 978-1-4244-5394-8. DOI: 10.1109/IPEC.2010.5542122.

[22] ADAMOWICZ, M. LCCT-Z-Source inverters. In: *10th International Conference on Environment and Electrical Engineering*. Rome: IEEE, 2011, pp. 1–6. ISBN 978-1-4244-8779-0. DOI: 10.1109/EEEIC.2011.5874799.

[23] MISHRA, S., R. ADDA and A. JOSHI. Inverse Watkins–Johnson Topology-Based Inverter. *IEEE Transactions on Power Electronics*. 2012, vol. 27, iss. 3, pp. 1066–1070. ISSN 1941-0107. DOI: 10.1109/TPEL.2011.2177278.

[24] MISHRA, S., R. ADDA and A. JOSHI. Switched-boost inverter based on Inverse Watkins-Johnson topology. In: *IEEE Energy Conversion Congress and Exposition*. Phoenix: IEEE, 2011, pp. 4208–4211. ISBN 978-1-4577-0542-7. DOI: 10.1109/ECCE.2011.6064343.

[25] NAG, S. S. and S. MISHRA. Current-Fed Switched Inverter. *IEEE Transactions*

on Industrial Electronics. 2014, vol. 61, iss. 9, pp. 4680–4690. ISSN 0278-0046. DOI: 10.1109/TIE.2013.2289907.

[26] ADDA, R., O. RAY, S. K. MISHRA and A. JOSHI. Synchronous-Reference-Frame-Based Control of Switched Boost Inverter for Standalone DC Nanogrid Applications. *IEEE Transactions on Power Electronics*. 2013, vol. 28, iss. 3, pp. 1219–1233. ISSN 1941-0107. DOI: 10.1109/TPEL.2012.2211039.

[27] RAVINDRANATH, A., S. K. MISHRA and A. JOSHI. Analysis and PWM Control of Switched Boost Inverter. *IEEE Transactions on Industrial Electronics*. 2013, vol. 60, iss. 12, pp. 5593–5602. ISSN 1557-9948. DOI: 10.1109/TIE.2012.2230595.

[28] NGUYEN, M.-K., T.-V. LE, S.-J. PARK and Y.-C. LIM. A Class of Quasi-Switched Boost Inverters. *IEEE Transactions on Industrial Electronics*. 2015, vol. 62, iss. 3, pp. 1526–1536. ISSN 1557-9948. DOI: 10.1109/TIE.2014.2341564.

[29] NAG, S. S. and S. MISHRA. A Coupled Inductor Based High Boost Inverter with Sub-unity Turns-Ratio Range. *IEEE Transactions on Power Electronics*. 2016, vol. 31, iss. 11, pp. 7534–7543. ISSN 1941-0107. DOI: 10.1109/TPEL.2016.2543499.

[30] CHUB, A., L. LIIVIK, J. ZAKIS and D. VINNIKON. Improved switched-inductor quasi-switched-boost inverter with low input current ripple. In: *56th International Scientific Conference on Power and Electrical Engineering of Riga Technical University (RTUCON)*. Riga: IEEE, 2015, pp. 1–6. ISBN 978-1-5090-0334-1. DOI: 10.1109/RTUCON.2015.7343171.

[31] HO, A.-V., T.-W. CHUN and H.-G. KIM. Extended Boost Active-Switched-Capacitor/Switched-Inductor Quasi-Z-Source Inverters. *IEEE Transactions on Power Electronics*. 2015, vol. 30, iss. 10, pp. 5681–5690. ISSN 1941-0107. DOI: 10.1109/TPEL.2014.2379651.

About Authors

Muhammad Awais SHARIF He received the B.Sc. degree in electrical engineering from the The Islamia University of Bahawalpur, Pakistan in 2016. He is currently working towards his M.S. Electrical Engineering degree in the National Fertilizer Corporation Institute of Engineering and Technology (NFC-IET) Multan, Pakistan. His research interests include, Power electronics,Power Inverters etc.

Muhammad SIDDIQUE was born in Multan, Pakistan. He received the B.Sc. degree in electrical engineering from the Bahauddin Zakariya University Multan, Pakistan in 2005. He received his M.Sc. degree in Power engineering from Pakistan Institute of Engineering and Applied Sciences Islamabad, Pakistan in 2007 and Ph.D. Degree from same institute in 2018. His research interests include, Power electronics, nonlinear control of power system, robust-adaptive control of systems, stability of time-delay systems, consensus control of multi-agent systems etc.

Muhammad Mubashir AKRAM He received the B.Sc. degree in electrical engineering from the National Fertilizer Corporation Institute of Engineering and Technology (NFC-IET) Multan, Pakistan in 2016. He is currently working towards his M.S. Electrical Engineering degree in the National Fertilizer Corporation Institute of Engineering and Technology (NFC-IET) Multan, Pakistan. His research interests include, Power electronics, Power Inverters etc.

Danish IQBAL He received the B.Sc. degree in electrical engineering from the National Fertilizer Corporation Institute of Engineering and Technology (NFC-IET) Multan, Pakistan in 2015. He is currently working towards his M.S. Electrical Engineering degree in the National Fertilizer Corporation Institute of Engineering and Technology (NFC-IET) Multan, Pakistan. His research interests include, Power electronics, Power Inverters etc.

Ghayyur HUSSAIN He received the B.Sc. degree in electrical engineering from the National Fertilizer Corporation Institute of Engineering and Technology (NFC-IET) Multan, Pakistan in 2016. He is currently working towards his M.S. Electrical Engineering degree in the National Fertilizer Corporation Institute of Engineering and Technology (NFC-IET) Multan, Pakistan. His research interests include, Power electronics, Power Inverters etc.

Muhammad Ali IMRAN He received the B.Sc. degree in electrical engineering from the National Fertilizer Corporation Institute of Engineering and Technology (NFC-IET) Multan, Pakistan in 2016. He is currently working towards his M.S. Electrical Engineering degree in the National Fertilizer Corporation Institute of Engineering and Technology (NFC-IET) Multan, Pakistan. His research interests include, Power electronics, Power Inverters etc.